Influence of cation vacancies and Bi impurity on the electronic structure and photoelectric properties of orthorhombic GeS

D. I. BLETSKAN[a,*], K. E. GLUKHOV[a], V. M. KABATSII[b]
[a]*Uzhhorod National University, Uzhhorod, Ukraine*
[b]*Mukachevo State University, Mukachevo, Ukraine*

Quantum-chemical studies of GeS electronic structure containing intrinsic point defects (vacancies in the cation (V_{Ge}) and anion (V_S) sublattices), isolated substitutional impurities Bi_{Ge} and {V_{Ge}–Bi_{Ge}}-type complexes were performed using density functional theory in the LDA+*U*-approximation as well as their role in the formation of photoelectric characteristics of the crystals was discussed. It was established that the localization of Bi impurity predominantly in the germanium positions induces the appearance of donor-type levels in the bandgap compensating the acceptor levels formed by cation vacancies which lead to the increase of dark resistivity as well as the sharp increase of photosensitivity of GeS crystals.
The features of chemical bonding in the defect-free and defective GeS crystals were analyzed on the basis of electronic density distribution maps. Electronic density maps clearly show the covalent-ionic bond nature within the corrugated double-layer packets with the predominant charge concentration on Ge–S (Bi–S) bonds as well as the weak van der Waals bond components between double-layer packets with the participation of germanium electronic lone pair.

(Received January 26, 2019; accepted October 9, 2019)

Keywords: Germanium monosulfide, Electronic structure, Point defects, Photoconductivity, Photoluminescence

1. Introduction

Great interest in layered crystals and thin layers of germanium monosulfide (GeS) is caused by the unique combination of their structure and physical properties that make them attractive to use as electric memory devices [1], as holographic recording media [2, 3], as photo-absorbing layers for the photovoltaic devices (solar cells) [4] as well as for the production of heterostructures by optical contact bonding [5], Schottky barriers [6], photoreceivers of linear polarized radiation [7], photoelectric sensors for the solar energy modules [8,9], optoelectronic sensors [10]. Photoelectric receivers of linear polarized radiation require the strongly anisotropic crystals that meet a number of requirements for ensuring the optimal values of operating device parameters: high photosensitivity in the specified spectral range, dark- and photoresistance, intertance, operating temperature range, etc.

Typical feature for germanium monosulfide is the nonstoichiometry which appears as a result of crystal structure regularity violation due to the presence of intrinsic point defects [11]. Cation vacancies (V_{Ge}) are ones of the most common types of intrinsic point defects in GeS crystals and their presence leads to significant changes of semiconductor properties of this nonstoichiometric compound in the homogeneity region. Besides intrinsic point defects, GeS crystals also contain the extended defects which are not related to crystal stoichiometry changes and represent the so-called layer packing defects [12].

The presence of a large number of intrinsic point (zero-dimensional) defects in GeS layered crystals determines the concentration of free charge carriers and the lifetime of minor charge carriers, i.e. ultimately the efficiency of optoelectronic devices created on their basis. The high concentration of intrinsic point defects (cation vacancies (V_{Ge})), which appearance are positively contributed by the one-sided homogeneity region [11], is the significant factor limiting the wider using of GeS layered crystals in modern photonics. Intrinsic defects, being electrically charged, form the *p*-type conductivity and high concentration (10^{17}–10^{18} cm^{-3}) of charge carriers (holes), which makes these crystals as low-impedance and slightly photosensitive.

The regulation of intrinsic point defects by donor impurity doping is an effective way to modify the physical macroscopic properties of GeS layered crystals. From a practical point of view, it is very important to obtain the maximum compensated crystals with a low concentration of charge carriers. For this purpose it is necessary to introduce into GeS such donor type impurity which would occupy the germanium vacancies and at the same time would partially neutralize the charge that will eventually leads to decreasing of holes concentration. Also, these impurities will increasing holes mobility by reducing the number of charged scattering centers, since the scattering of charge carriers (holes in this case) by the charged defects usually occurs much more intensively than by the neutral ones. Thus, it is possible to change not only the concentration of charge carriers by doping but also to identify the effects associated with the formation of deep

local levels in the bandgap of these crystals.

Earlier we established [13] that the doping of GeSe, which is isostructural to GeS, by the Bi donor impurity allows one to considerably modify its electrical and photoelectrical properties. The introduction of Bi atoms is accompanied by the "healing" of cation vacancies that causes a significant increase of photoconductivity.

The important information about the electronic characteristics of cation vacancies and bismuth impurity atoms at their interaction with the electrons of a matrix can be obtained from the theoretical calculations of electronic structure and experimental studies of impurity states from photoconductivity and photoluminescence spectra. It should be noted that by now the electronic structure of ideal defect-free stoichiometric GeS has been already studied using various band theory computational methods: semiempirical pseudopotential [14], linear combination of atomic orbitals (LCAO) [15], first-principle calculation method based on the density functional theory [16], Hartree-Fock and full-potential linearized augmented plane wave (FP-LAPW) methods [17]. A significant disadvantage of these works is an arbitrary choice of the setting and the notation system of crystal axes within the D_{2h}^{16} space group (*Pcmn* [14, 17], *Pmnb* [15], *Pnma* [16]) with a different matching of the axes to the Brillouin zone. It complicates the usage of available GeS band calculation results for the interpretation of experimental optical and photoelectrical spectra. Along with the theoretical studies, there are also experimental investigations of the features of GeS electronic states by the ultraviolet and X-ray photoelectron spectroscopy [18-25] as well as electron energy loss spectroscopy [26] methods.

Despite the fact that the band structure of defect-free GeS has been studied in detail, then the information about the influence of intrinsic and extrinsic point defects on the electron-energy characteristics of germanium monosulfide is comparatively poor. It is possible to point the only two known by us papers where GeS electronic structure calculations with germanium and sulfur vacancies were performed by a Green's functions method [27] and within density functional theory approach [28]. As regards to the Bi impurity influence, such calculations have not been performed yet. Therefore it is important to obtain more detailed information about the electronic characteristics of different intrinsic and extrinsic point defects as well as their interactions with the electronic subsystem of matrix.

This paper presents the quantum chemical investigation results of electronic structure for the defect-free germanium monosulfide as well as for the crystals containing germanium and sulfur vacancies, isolated substitutional impurity atoms Bi_{Ge} (Bi→Ge) and also vacancy-impurity complexes $\{V_{Ge}–Bi_{Ge}\}$. It is discussed the role of these defects in the formation of photoconductivity spectral characteristics. The energy bands, total and partial densities of states appears as the calculation results. The charge density maps were used for the illustration of individual interatomic interactions.

2. Crystals preparation of and their structure

2.1. Crystal growth

Specially undoped and Bi-doped GeS single crystals were grown by the static sublimation method in the sealed quartz ampoules pre-evacuated down to the pressure 0.133 Pa with 18-22 mm internal diameter and 180-200 mm length. The synthesis of initial polycrystalline substance was carried out by a direct fusion of elementary components (germanium with the specific resistance 50 Ohm·cm and sulfur with the purity HP V-5) taken in the stoichiometric ratio. It is known that the maximum melting temperature for the $A^{IV}B^{VI}$-type compounds does not correspond to the stoichiometric composition, therefore they are considered as the compounds with shifted stoichiometry. The domain of homogeneity of GeS is fully situated in the excess sulfur region (relative to the stoichiometric compound) [11]. Sulfur content increasing in GeS crystals under the closed volume conditions can be explained by the fact that any composition tends to the free energy minimum, therefore the alloys with the highest possible relative chalcogen content are preferred for GeS–S solid solution. Numerous experiments have shown that the usual fusion of elementary components in the stoichiometry quantities leads to composition shift into the homogeneity region. Attempts to obtain the crystals with stoichiometry composition by the introducing of Ge superstoichiometry excess (in the various quantities) as well as by the varying of growth conditions were unsuccessful, though approached the composition closer to the stoichiometry. Therefore the real GeS crystals always contain germanium vacancies.

GeS:Bi crystals were grown in order to verify the consequences obtained as results of quantum-chemical modeling of the electronic structure of bismuth-doped germanium monosulfide. The doped crystals were obtained as follows: metallic bismuth in an amount 0.1 and 1.0 at. % was added into the initial furnace charge before synthesis start and the synthesis process was carried out together with the impurity. After synthesis finish the obtained polycrystalline ingot was shaken off into one ampoule end and then it has been placed in the horizontal two-zone tubular furnace of resistive heating. The optimum crystal growth conditions are followed: the temperature of evaporation zone is 900 K; the temperature of condensation zone is 800 K. Crystals from the gas phase were grown in the form of plane-parallel plates with the dimensions up to 8×15×0.1 mm. The layered structure character explains the lamellar habit of GeS crystals with well-developed faces (001).

2.2. Crystal structure

Germanium monosulfide crystallizes in the orthorhombic structure with the lattice parameters $\boldsymbol{a}$ = 4.299 Å, $\boldsymbol{b}$ = 3.646 Å, $\boldsymbol{c}$ = 10.481 Å, Z = 4, its symmetry is described by D_{2h}^{16} (*Pcmn*) space group [29]. GeS structure is a derivative of black phosphorus structure, the half of atoms of its orthorhombic cell is replaced by Ge atoms and

the second half by S atoms (Fig. 1, *a*).

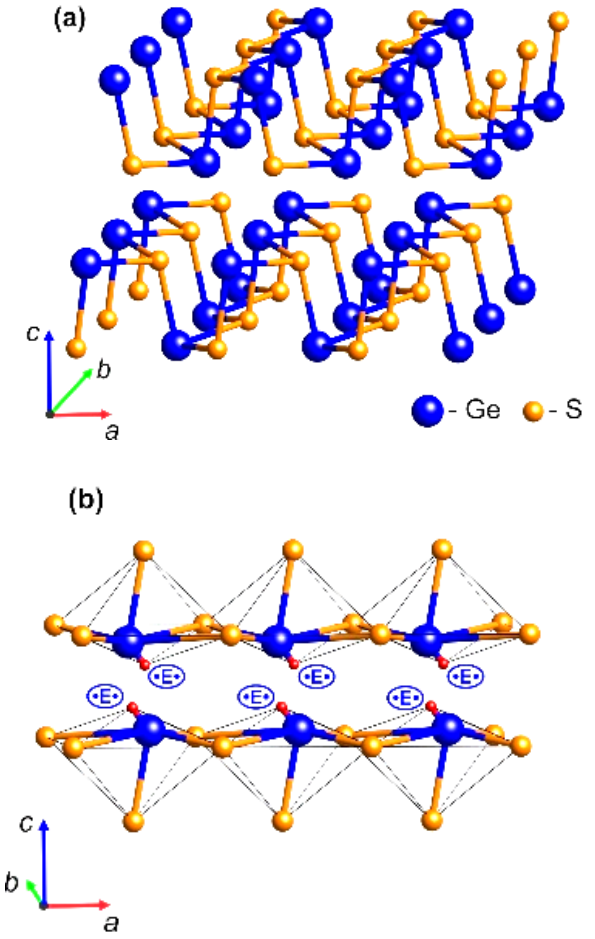

Fig. 1. Crystal structure (a) and ψ-octahedra [GeS_5•E•] packing (b) in the orthorhombic GeS phase (•E• – electronic lone pair)

The electronic configurations of valence electrons for germanium and sulfur atoms are $3d^{10}4s^24p^2$ and $3s^23p^4$ respectively. Sulfur is a more electronegative element in GeS compound, so it takes two electrons from the germanium atom, which leads to the electronic configuration $3s^23p^6$ for S^{2+} and $3d^{10}4s^24p^0$ for Ge^{2-}. Thus, the germanium oxidation state in GeS is equal II (2+). In this state, two 4*p*-electrons of germanium participate in the chemical bond formation while two 4*s*-electrons forming the lone pair. This electronic lone pair is not directly involved in the chemical bond formation, but it significantly affects the asymmetrical arrangement of sulfur atoms around germanium atom that finally leads to the formation of distorted ψ-octahedra [GeS_5•E•], where •E• is the electronic lone pair. These coordinating ψ-octahedra of Ge atoms are edge-connected to each other and form the corrugated double-layer packets in the XY plane (Fig. 1, *b*). Double-layer packets are packed along the ***c*** axis and connected together by the weak van der Waals forces while the ionic-covalent bond type acts inside the double-layer packets.

3. Calculation method

At the present time, the supercell model with the application of *ab initio* electronic structure calculation methods [30] is most effectively used for the description of the electronic structure of defect crystals. We performed the electronic structure calculations in the framework of density functional theory using the basic sets of plane waves (PW), linearized combination of atomic orbitals (LCAO) and norm-conserving pseudopotentials, as realized in the SIESTA and ABINIT [31-34] software packets. The first-principle atomic norm-conserving pseudopotentials [36,37] were used in the calculations with electronic configurations: [Ar] $4s^24p^2$ for Ge atoms, [Ne] $3s^23p^2$ for S atoms, [Kr] $6s^26p^3$ for Bi atoms. The specified states belong to the valence shells and [Ar], [Ne], [Kr] – to the core. It is well-known that the first-principle calculations within the density functional theory in the local density approximation (LDA) for the exchange-correlation potential give the underestimated value of the bandgap. The accounting of direct Coulomb single-site interaction *U* within the Hubbard model [37] can significantly affect the value of fundamental band gap width, the depth of defect states in the bandgap as well as the charge localization. Therefore, the LDA+*U*-approximation in comparison with the LDA-calculations were used in the present work for a correct description of electronic correlations [38, 39].

The 2×2×1 supercell was used in our calculations; it was obtained by the double translation of germanium monosulfide orthorhombic primitive cell along the directions of crystallographic ***a*** and ***b*** axes. The choice of such a cell is optimal because it allows one to carry out a structural relaxation of nearest atoms without the essential increase of computation time. The supercell model using suggests the impurity ordering in the calculation whereas the disordering effects in the real-doped crystals significantly affect their photoelectric properties. Modeling of vacancies in the supercell contained 32 atoms supposes the removing one of germanium or sulfur atoms as well as the impurity case supposes the introduction of one Bi atom into the supercell instead of one Ge atom. The relaxation procedure of supercell geometry (preserving the overall crystal symmetry) was performed for each considered defect configurations to achieve the total energy minimum E_{tot} and the force values acting on the ions less than 0.01 eV/Å.

The Ge and S atom positions in the corrugated monolayer plane of a double-layer packet of GeS crystal with germanium vacancy and Bi_{Ge} substitutional impurity after the structure relaxation are shown in Fig. 2. As can be seen from this figure, in the case of germanium vacancy presence it occurs the displacements of sulfur atoms nearest to a vacancy in the direction away from the vacancy position by 0.29–0.34 Å after relaxation, however, the local arrangement of nearest and subsequent next to the nearest atoms does not change significantly.

The displacements of S atoms away from V_{Ge} vacancy positions is caused by the fact that the removing of germanium ion leads to the increasing of repulsion

between the S ions which are nearest to the vacancy as well as it also increases the Coulomb attraction of these ions to the germanium ions located in the second coordination sphere. The modeling of Bi→Ge substitutional impurity relaxation is accompanied by radial displacement of the nearest sulfur atoms in the direction to the impurity center (Fig. 2, *c*) and the substitution energy has a positive sign.

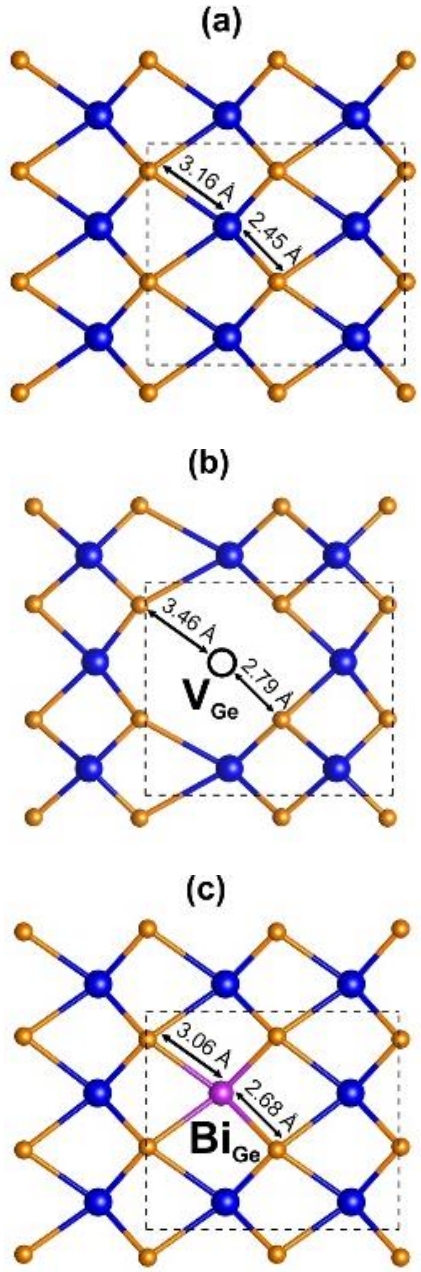

Fig. 2. The local atomic structure of defect-free GeS crystal (a) as well as crystal with the presence of germanium vacancy (b) and bismuth impurity (c) after relaxation

4. Results and discussion

4.1. Electronic structure and density of states of defect-free stoichiometric GeS

At first, we performed the electronic structure calculations of defect-free GeS crystal. Considering that the crystallographic ***a*** and ***b*** axes of real GeS crystals are in the planes of double-layer packets and ***c*** axis is perpendicular to them, then the choice of *Pcmn* setting of the D_{2h}^{16} space group for the band structure calculations is correct. It allows one to carry out a more reliable interpretation of the observed features in the experimental optical and photoelectric spectra on the basis of the calculated electronic structure.

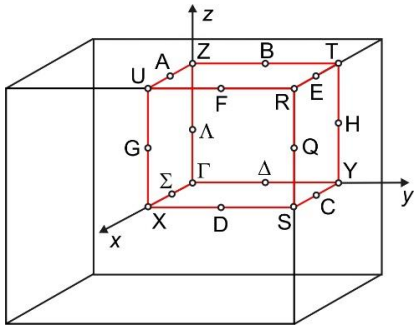

Fig. 3. The Brillouin zone of orthorhombic GeS

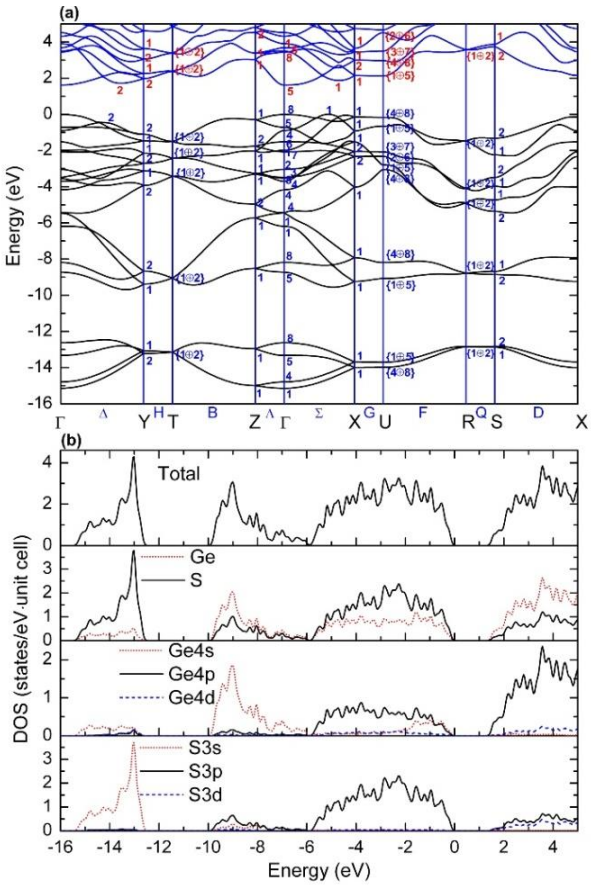

Fig. 4. Electronic structure (a), total and local partial density of states (b) of GeS crystal

The structure of energy bands of defect-free orthorhombic GeS crystal calculated by the density functional method without regard for the spin-orbital interaction in the LDA+*U* approximation in all high symmetry points (Γ, Y, T, Z, X, U, R, S) and along symmetric directions of the Brillouin zone (Fig. 3) is shown in Fig. 4, *a* where the energy origin is placed at the last occupied state. The indices at the Γ, Y, T, Z, X, U, R, S, Σ, Δ letters denote the irreducible representations.

According to our calculations in the LDA+*U*-approximation, the defect-free GeS is an indirect-gap semiconductor with the calculated bandgap width E_{gi} = 1.61 eV (transition $\Sigma_1 \rightarrow \Gamma_5$) as well as with the direct gap E_{gd} = 1.63 eV (transition $\Gamma_8 \rightarrow \Gamma_5$).

The valence band of defect-free stoichiometric GeS has the total width 15.14 eV (from the bottom edge of S3*s*-band to the valence band top) and contains 20 dispersive branches which are divided into three subbands (VBI, VBII, VBIII) by the nature of states. Information about the atomic orbital contributions into the crystal states of these subbands is provided by the calculations of total $N(E)$ and local partial $n_{at}(E)$ densities of states (Fig. 4, *b*). The quasi-core bands (VBIII) forming the valence band bottom in the energy interval from –15.14 to –12.62 eV are composed mainly by atomic S3*s*-orbitals with the insignificant impurity of germanium 4*s*- and 4*p*-states. The middle VBII subband (from –9.68 to – 5.46 eV) is separated from the bottom subband by the forbidden gap and it is formed as a result of the overlapping of Ge4*s*-S3*p*-states, wherein Ge4*s*-states of the electronic lone pair make the greater contribution to the formation of this subband. The uppermost valence subband VBI (from – 5.45 eV to the valence band top) has the mixed character with the participation of hybridized germanium 4*p*-, 4*s*-states, and sulfur 3*p*-states. The characteristic feature of germanium monosulfide electronic spectrum is a significant contribution of Ge4*s*-states of the electronic lone pair in the formation of valence band top. The electronic low-energy structure of the unoccupied electronic states of germanium monosulfide is formed mainly by the mixing of free *p*-states of germanium and sulfur with a minor contribution of *d*-states of both components.

The necessary condition which allows comparing the results for defective supercells is a reliable transfer of the bulk properties of defect-free crystal by the supercell model. For this purpose, we performed the electronic structure calculations of defect-free crystal in the supercell model using the LDA+*U*-approximation (Fig. 5, *a*, *b*).

Only four high-symmetry points of the Brillouin zone namely Γ(0, 0, 0), X(0.5, 0, 0), Y(0, 0.5, 0), Z (0, 0, 0.5) were used for the band structure calculations of defective crystals in the supercell model, however some calculations were tested using eight points for the determination of result reliability.

It follows from the comparison of electronic band structures and densities of states of a defect-free GeS crystal calculated in the single unit cell (Fig. 4, *a*, *b*) and in the supercell (Fig. 5, *a*, *b*) models, that they do not essentially differ both by the subband quantity and their formation genesis.

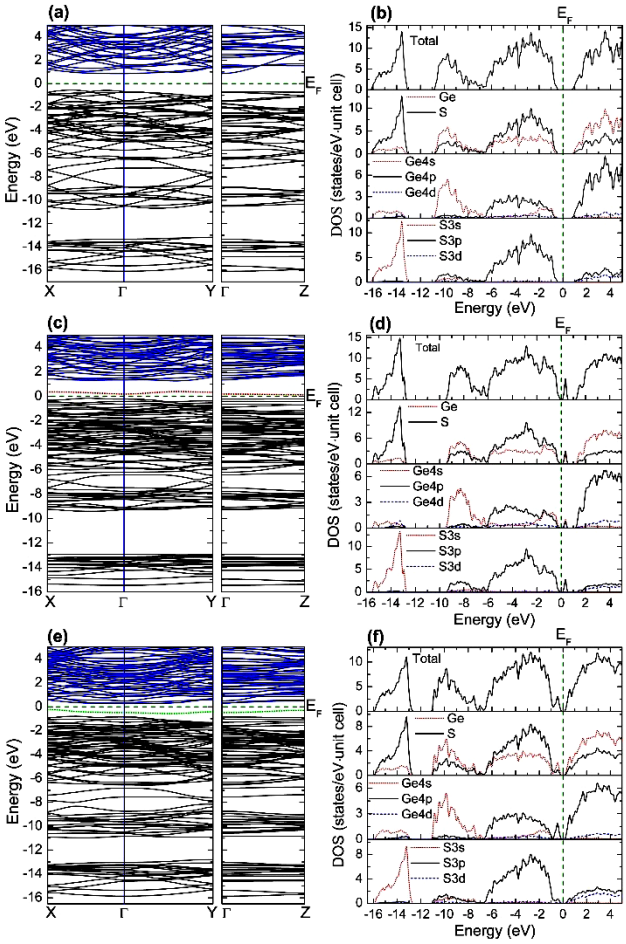

Fig. 5. Band structure, total and local partial densities of states of defect-free GeS crystal (a, b), GeS with cation (c, d) and anion (e, f) vacancies in the supercell model 2×2×1

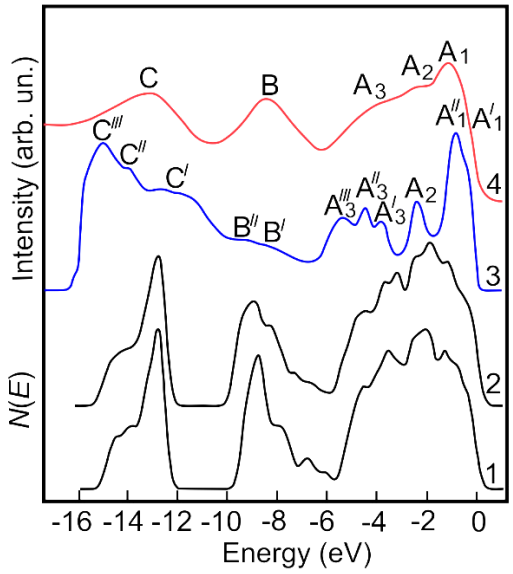

Fig. 6. Comparison of the LDA+U calculated the total density of states of valence band in the unit-cell (1) and supercell (2) models with the experimental UPS (curve 3, 21.2 eV), XPS (curve 4, 1486.6 eV) spectra [14] of GeS crystal

Adequacy of the model description of defect-free GeS electronic structure in the unit cell and supercell band calculations can be confirmed from the similarity of calculated total densities of states and experimental photoelectron spectra. The total densities of states $N(E)$ of defect-free germanium monosulfide obtained by the unit cell and supercell band calculations are compared in the unified energy scale in Fig. 6 with the known experimental X-ray and ultraviolet photoelectron spectra of GeS crystal taken from Ref. [14]. This figure shows that both calculations reproduce well the centroid (peak) positions of energy bands in the experimental XPS and UPS spectra. This result is very important because the traditional semiempirical electronic structure calculation methods are unsuitable for the studying of defective crystals and crystals containing substitutional impurities, thus, in this case, it is expedient to use a supercell model.

4.2. GeS with cation and anion vacancies

The presence of lattice vacancies in the ideal crystal leads not only to the modification of its local geometry, but it is also reflected primarily on the electronic properties of whole crystal and ions near the defect in particular. The electronic structure of defective GeS crystal with germanium sublattice vacancies is shown in Fig 4, *c* as well as the total and partial densities of states – in Fig. 4, *d*. For the calculation result analysis of defective crystal electronic structure, it is important to separate the defect states from the crystal matrix states, since the presence of V_{Ge} and V_S vacancies leads not only to the shift of whole electronic energy spectrum and Fermi level E_F, but also to the transformation of entire electronic energy spectrum.

The studying of electronic states of isolated cation vacancies in GeS has shown that vacancy states (mainly *s*-symmetry) are located in the valence band depth near S3s-band top (Fig. 4, *d*). Their genesis is caused by the rearrangement of electronic states of the matrix, and the wave functions of sulfur atoms closest to the cation vacancy are playing here the defining role. Besides, the acceptor level formed by sulfur 3*p*-states and germanium 4*s*-, 4*p*-states appears at 0.34 eV above the valence band top in the band spectrum of nonstoichiometric GeS:V_{Ge}. The similar value of acceptor level occurrence depth $\Delta E_A = 0.27$ eV for defective GeS crystal was obtained in Ref. [27], where the calculations using the Green's functions method were performed.

The band structure and the energy distribution of density of states of GeS with sulfur vacancy are shown in Fig. 4, *e* and *f*, respectively. The presence of sulfur vacancy does not lead to the forming of embedded states in the depth of valence band, but in the fundamental gap below the conduction band bottom, it appears a deep donor level $\Delta E_D = 0.64$ eV formed by *p*-orbitals of germanium atoms surrounding sulfur vacancy. The fact that anion vacancy leads to the formation of a deeper local level in the fundamental gap than the cation vacancy is explained by the stronger potential of this defect, which is also pointed out in Ref. [27]. At the same time, it is necessary to point out the fact that the presence of sulfur vacancies as the main type of defects in germanium monosulfide is unlikely because it would lead to the *n*-type conductivity of these crystals whereas the specially undoped GeS crystals regardless the growth method always are the *p*-type conductivity.

4.3. The modification of germanium monosulfide electronic structure by the substitution Bi→Ge impurity

The introduction of Bi impurity atoms into germanium monosulfide can significantly affect its electronic structure, conductivity, photoconductivity, and other properties. This influence considerably depends on: 1) the position of introduced impurity atom in the matrix crystal lattice; 2) the natural atomic point defects which concentration considerably varies with the introduction of impurity atoms; 3) the association between the impurity atom and the intrinsic atomic point defects. We have considered two most probable variants of the introducing of Bi impurity atoms into GeS crystal matrix: the cation substitution (Bi atom in the cation positions Bi_{Ge}) and the formation of complexes of «cation vacancy – impurity atom» {V_{Ge}–Bi_{Ge}}-type.

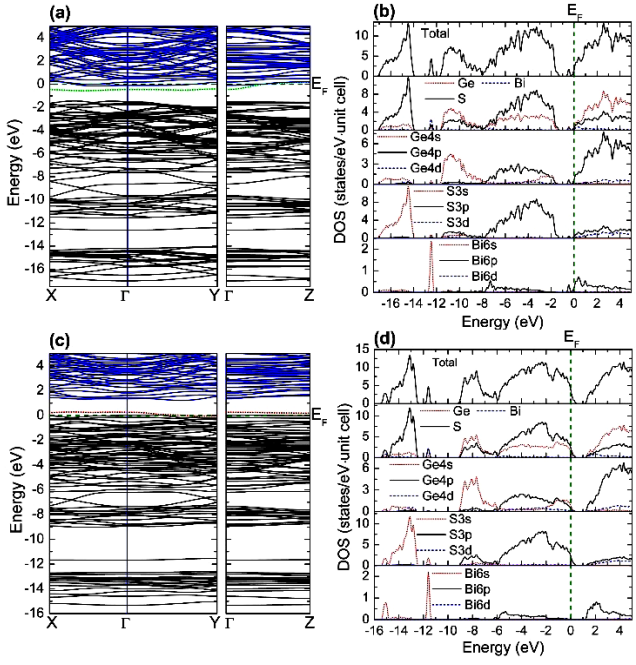

Fig. 7. Band structure, total and local partial density of states of GeS crystal with the cation substitutional impurity Bi_{Ge} (a, b) as well as with the {V_{Ge}–Bi_{Ge}} defect type (c, d) in 2×2×1 supercell model

The prevailing mechanism of bismuth doping effect in GeS at low impurity concentration (≤0.1 at. %) is the filling of cation sublattice by Bi^+ ions. We will consider the total and partial densities of states (Fig. 7, *b*) for the analysis of the changes of GeS:Bi electronic structure (Fig. 7, *a*) caused by the substitution effect in germanium sublattice (Bi→Ge). The energy positions, as well as the

widths of valence band and conduction band, are almost not undergoing significant changes at the transition from the defect-free crystal to the doped one. Thus, Bi→Ge substitution does not change the semiconductive properties of the matrix: all binding states are occupied, the conduction band is empty, and the energy gap is slightly decreasing. The main feature of the electronic structure of bismuth-doped germanium monosulfide is the appearance of new states in the valence band depth: one below S3*s*-band and other in the gap between occupied S3*s*- and Ge4*s*+S3*p*-bands. These states appear due to the interaction of Bi6*s*-orbitals with 3*s*-orbitals of the closest sulfur atoms. Fermi's level is placed near the conduction band bottom at Bi→Ge substitution. There is a donor level in the forbidden gap below the Fermi's level with a depth 0.32 eV below the conduction band bottom.

4.4. Defect of {V_{Ge}–Bi_{Ge}}-type

It is necessary to take into account the interaction between the introduced impurity defects with the intrinsic crystal point defects for the analysis of properties of GeS doped crystals. The increasing of concentration of electrically active bismuth impurity introduced into GeS crystals leads to the increase of solubility of intrinsic point defects of crystal lattice compensating the impurity doping effect that is the self-compensation phenomenon occurs. Along with the single cation vacancies, the formation of complexes consisting of impurity atoms and vacancies can significantly reduce the energy of defect formation and therefore it can significantly increase the self-compensation effect. In this case, the character of the dependence of the concentration of current carriers on the content of the dopant also changes, which ultimately affects the value of dark conductivity and impurity photoconductivity.

The changes of the electronic structure at the simultaneous presence of two defect types, cation sublattice vacancies (V_{Ge}) and substitutional defect of bismuth atom at germanium atom site (Bi_{Ge}) were considered for the supercell of $Ge_{0.875}Bi_{0.0625}V^{Ge}_{0.0625}S$ composition. Fig. 6, *c* and *d* present the electronic structure, total and partial densities of states for this {V_{Ge}–Bi_{Ge}} complex configuration. The simultaneously presence of two types of lattice defects (structural vacancies and substitutional impurity {V_{Ge}–Bi_{Ge}}) in the germanium monosulfide crystal lattice causes the appearance in the gap between the occupied states of lowermost S3*s*-band and middle Ge4*s*+S3*p*-band two embedded states (Fig. 7, *c*, *d*). Such states are specific for the electronic structures with the presence of only V_{Ge} cation vacancy or only Bi_{Ge} substitutional impurity. The local impurity level of acceptor type with the depth ΔE_A = 0.1 eV is formed in the band gap near the valence band top. Thus, the electronic structure modeling of germanium monosulfide with the presence of {V_{Ge}–Bi_{Ge}} defect type should not lead to the conductivity type inversion, which is confirmed experimentally.

4.5. Electronic density maps

The mechanism of chemical bonding formation in the defect-free and defective germanium monosulfide can be analyzed in details by considering the electronic density contour maps constructed on the basis of DFT calculations in the supercell model. Figs. 8 and 9 show the calculation results of valence electron charge density distribution of the ideal GeS crystal as well as the crystal containing cation and anion vacancies, substitutional impurities (Bi→Ge) in the form of electronic density maps for two characteristic crystallographic planes (001) and (010).

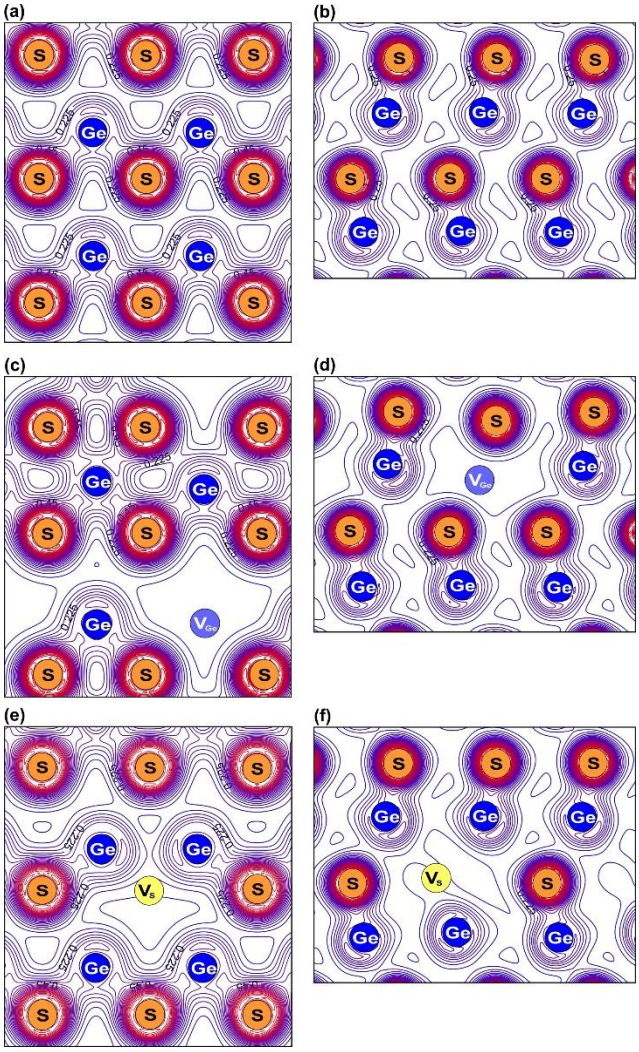

Fig. 8. Spatial distribution maps of valence electronic charge density for the defect-free GeS crystal (a, b) as well as for GeS with a germanium vacancy (c, d) and with a sulfur vacancy (e, f) built in (001) (a, c, e) and (010) (b, d, f) planes

Interatomic interactions in the defect-free GeS have the combined character and include ionic, covalent and weak van der Waals components. From Fig. 8 it can be seen that the charge density concentrates mainly within the corrugated double-layer packets. From the maps, it is also visible that there are localized maxima on the Ge–S bonds, which are combined together by the overall contours. A

strongly pronounced deformation of contours ρ(**r**) from sulfur atoms toward germanium atoms along the Ge–S bond line and the existence of the common contours encompassing the maxima of electron density over the cation-anion bonds (Fig. 8, *a* and *b*) characterize the covalent component of the chemical bond. The presence of the covalent bond component is caused by the hybridization of 4*p*-states of germanium and 3*p*-states of sulfur (Fig. 3, *b*).

The ionic bond component is determined by the partial transfer of charge density from germanium atoms to sulfur atoms due to the difference of their electronegativities ($EN^{(Ge)}$ = 2.01, $EN^{(S)}$ = 2.58). Thus, electronic density maps are characterized by the higher valence electron density in the vicinity of sulfur sites.

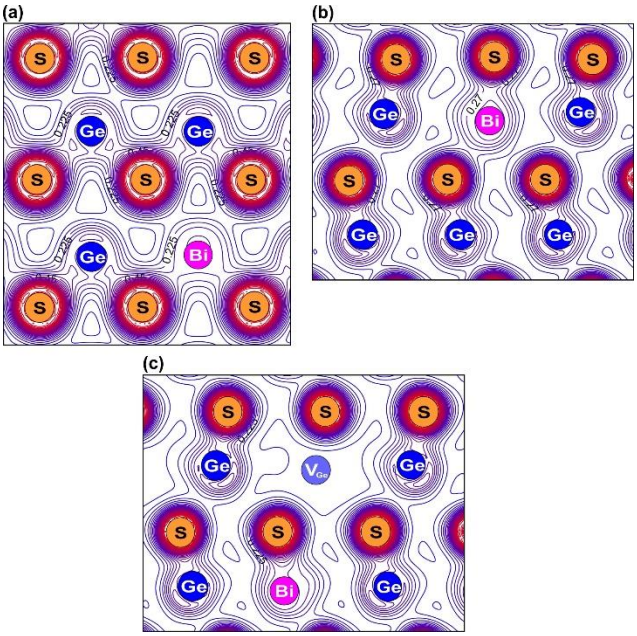

Fig. 9. Spatial distribution maps of valence charge density for GeS crystal with Bi_{Ge} substitutional impurity (a, b) and with a complex of {V_{Ge}–Bi_{Ge}}-type in (001) (a) and (010) (b, c) planes

Thus, the charge density in germanium monosulfide concentrates mainly within the corrugated two-layer packets while the electron density between packets is minimal which reflects the layered character of the crystal structure of this compound. The presence of an insignificant overlap of the wave functions related to the atoms of the nearest-neighbor double-layer packets is caused by the states of electronic lone pair (•E•) of germanium directed toward the interlayer van der Waals gap (Fig. 8, b).

Using charge density maps it is also convenient to study the changes of total electronic density distribution caused by the cation (anion) removal and the vacancies formation or by the substitution atom introduction. According to the calculation results (Fig. 8, *c*–*e*), the chemical bonds which had been broken at the removal of germanium (sulfur) atoms from the lattice site, are not restored with the formation of new covalent bonds through the vacancy, i.e. there are no "bridges" between the atoms nearest to the vacancy and the vacancy itself (V_{Ge}, V_S). From Fig. 8, it is clear that the significant contour changes occur near vacancies.

From these figures, it can be seen that the electronic density ρ(**r**) distribution in the V_{Ge} (V_S) vacancy sites has a delocalized character. From the shape of the total charge distribution, one may conclude that in the presence of cation (V_{Ge}) or anion (V_S) vacancies the electronic densities of at least two coordination spheres of the atoms are perturbed. The perturbing mechanism of Ge-vacancy is related to the changes of electronic states of sulfur atoms nearest to V_{Ge}. The part of S3*p*-states transfers into the region of nonbonding states. As a result of the presence of Ge-vacancies, there is an "emptying" of some part of bonding states, and the Fermi's level E_F shifts down in the energy scale.

The presence of ionic chemical bond component and the associated possibility of separating the electropositive and electronegative components from the binary semiconductor GeS compound lead to necessity the localization of Bi impurity atoms in the cation sublattice.

Since the electronic density maps of crystals show the change of electron distribution at the formation of chemical bonds between the matrix atoms (base substance) and impurity atoms, so they can serve as an evident illustration of individual interatomic interactions. As it was mentioned in Sec 4.3, the doping of GeS cation sublattice by Bi impurity leads to appear the fairly deep levels in the matrix electronic structure which correspond to the electronic states localized on bismuth atom and nearest sulfur atoms. It testifies the occurrence of strong chemical bonding between bismuth and sulfur atoms. It is possible to establish the nature of these bonds by electronic charge spatial distribution analysis. The contours ρ(**r**) between bismuth impurity and sulfur atoms (Fig. 9) are similar to the contours of cation and anion in the main matrix that testifies the strong chemical interaction between metal impurity atom and chalcogen atoms. The contours ρ(**r**) near Bi impurity (Fig. 9) indicate the existence of a covalent bonding component in the Bi–S bonds. The main role of covalent bonding between bismuth impurity and nearest sulfur atoms plays S3*p*-Bi6*p* interaction.

5. Photoconductivity spectra of GeS crystals

5.1. Measurement technique

For measurements of dark conductivity and photoconductivity, the coplanar contacts by indium fusing or aquadag coating were deposited on (001) natural crystal faces, so that electric field was applied along the crystallographic ***b*** axis. The ohmic character of contacts was confirmed by the linearity of the VAC both under light as well as in the dark. According to the thermo-EMF sign it is found that both intentionally undoped and bismuth-doped GeS crystals had *p*-type conductivity.

The measurements of PC spectra were carried out under constant electric field conditions (which did not

exceed 5 V/cm) at 100 K and 293 K in the wavelength range from 0.4 to 2.5 microns, under the illumination of samples by the monochromatic intensity-modulated radiation with the modulation frequency 130 Hz. The light pulse duration at the used frequency was much longer than the generation and relaxation time of nonequilibrium charge carriers. The modulated light beam exited from the monochromator was passed through a polarizer (Glan's prism) and then it was incident normally on (001) surface of the studied samples. The light probe width did not exceed 0.5 mm. Since two crystallographic ***a***, ***b*** axes are located in the (001) plane it was possible to investigate the anisotropy of PC spectra in the layer plane. Let's notice, that in most cases the anisotropy of physical properties of layered crystals is examined only along and across the layers.

5.2. Photoconductivity spectra of intentionally undoped GeS crystals

Intentionally undoped GeS crystals regardless of growing method contain germanium vacancies, have *p*-type conductivity, are low-impedance (specific dark resistance ρ_d = 10^2–10^3 Ohm·cm) and poorly photosensitive. Photosensitivity spectra show a strong dependence on the spatial orientation of the polarization plane of incident radiation (curves 1, 2 in Fig. 10) when the intentionally undoped GeS crystals are illuminated by monochromatic linearly polarized radiation (LPR) in the normal direction (i.e. along ***c*** axis) to the illuminated surface (001). From the comparison of polarized photoconductivity spectra and edge absorption (curves 3, 4 in Fig. 10) measured at T = 293 K, it follows that the energy positions of photosensitivity maxima correspond to the value of absorption coefficient $\alpha = 10^3$ cm^{-1}, i.e. both maxima are intrinsic. The extrema positions in the polarized PC spectra are entirely determined by the spatial orientation of the main crystallographic ***a*** and ***b*** axes in the (001) plane. Taking into account the results of band structure calculation (Fig. 4, *a*) we can conclude that the long-wave component of photoactive absorption (with a maximum $h\nu_{max1}$ = 1.65 eV) (curve 1 in Fig. 10) dominates in the ***E*** || ***a*** polarization (transition $\Sigma_1 \rightarrow \Gamma_5$). In the ***E*** || ***b*** polarization the photosensitivity prevails in more short-wave spectral region with a maximum $h\nu_{max2}$ = 1.75 eV (curve 2 in Fig. 10) and is connected with the optical transition $\Sigma_1 \rightarrow \Delta_2$.

Both intrinsic maxima in the polarized PC spectra are shifted together with the fundamental absorption edge toward the short-wave region with the sample temperature decreasing, thus it reflects the increasing of GeS bandgap width. Two strongly polarized high-energy bands $h\nu_{max}$ = 2.2 eV for ***E*** || ***a*** and $h\nu_{max}$ = 2.18 eV for ***E*** || ***b*** appear in the PC spectra at T = 90 K (curves 1 and 2 in Fig. 11) caused by the optical transitions from the deeper states of valence band to the conduction band. The wide photosensitivity spectral region in the depths of fundamental absorption of GeS layered crystals with natural faces (Fig. 11) grown by a sublimation method shows a low surface recombination rate, which is typical for the vast majority of layered semiconductors.

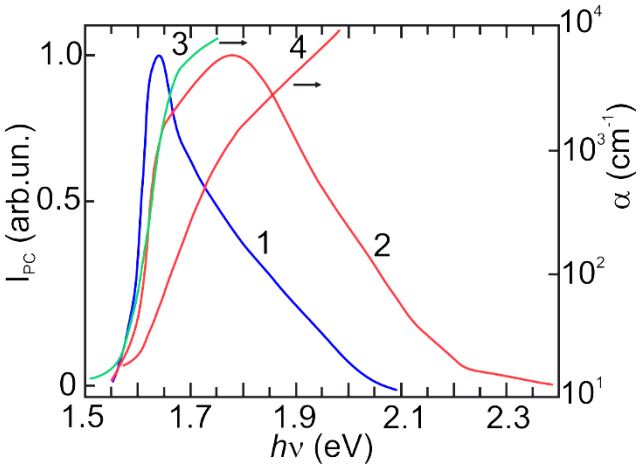

Fig. 10. Polarized photoconductivity (1, 2) and edge absorption [40] (3, 4) spectra of GeS crystal grown by sublimation:
*1, 3 – **E** || **a**, 2, 4 – **E** || **b**. T = 293 K*

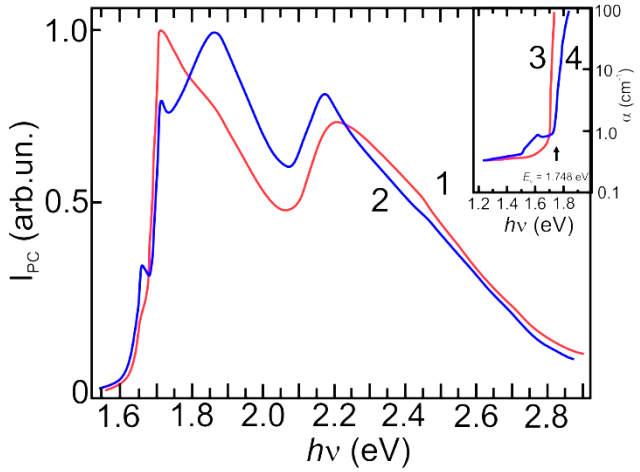

*Fig. 11. Polarized photoconductivity spectra of GeS crystal grown by sublimation:1 – **E** || **a**, 2 – **E** || **b**. T = 90 K. The inset shows the polarized edge absorption spectra taken from Ref. [41]: 3 – **E** || **a**, 4 – **E** || **b**. T = 4.2 K*

Also, PC spectra of intentionally undoped GeS crystals at low temperatures have the feature in the influx form in ***E*** || ***a*** polarization and a narrow maximum with $h\nu_{max}$ = 1.65 eV in ***E*** || ***b*** polarization (curves 1 and 2 in Fig. 11) on the long-wave decline. Taking into account the electronic structure of GeS with cation vacancies (Fig. 5, *c*) and the fact that real germanium monosulfide crystals always contain germanium vacancies we associate the peak at 1.65 eV with the optical transitions of electrons from the valence band to the acceptor level formed by these vacancies. Optical absorption experiments provide direct information on the energy spectrum of impurity states. The appearance of local energy level between the conduction band bottom and the valence band top (Fig. 5) in GeS crystals containing cation vacancies should lead to the occurrence of absorption band in the energy range, less than the bandgap width. Really, as was shown by the authors [41], at low temperatures, an impurity band is

observed in the absorption-edge spectra of GeS crystal (insert in Fig. 11). The energy position of this maximum, taking into account its temperature shift, corresponds to the maximum which we observed on the long-wave decline of the intrinsic PC (Fig. 11, curve 2).

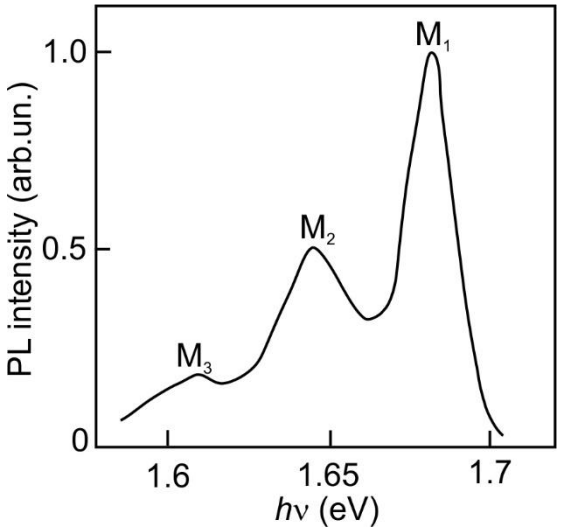

Fig. 12. Photoluminescence spectra of GeS crystal T = 4.2 K

Photoluminescence (PL) spectroscopy is another independent method to study the localized states in the bandgap of semiconductors. Low-temperature near-edge photoluminescence spectrum obtained by exciting the intentionally undoped GeS crystals with He-Ne laser (6328 Å) is shown in Fig. 12. The spectrum of radiative recombination at T = 4.2 K consist of a series of equidistant M_1 (1.682 eV), M_2 (1.646 eV) and M_3 (1.610 eV) bands. As the sample temperature increases above 10 K then the band intensities decrease (i.e. it is observed their temperature quenching) so these bands cannot be observed above 40 K. The most intensive near-edge M_1 band in PL spectra of GeS crystals is caused by the radiative recombination involving cation vacancies and M_2, M_3 bands are the phonon replicas of M_1 band.

5.3. Bi impurity influence on the photo-conductivity spectra of GeS crystals

Doping of germanium monosulfide by Bi donor impurity within the solubility region leads to the significant increase of the specific dark resistivity ($\rho_t = 10^6$–10^7 Ohm·cm), thus it is not observed the inversion of conductivity type and the crystals are *p*-type conductivity. The self-compensation of donors by intrinsic defects (Ge vacancies) in GeS:Bi crystals at small impurity concentration is observed; it concluded that the formation of intrinsic lattice defects that gives the charge carriers of opposite sign at the introduction of electrically active Bi impurity into the crystal becomes energetically favorable. At the same time, the self-compensation of electrically active impact of Bi impurity in germanium monosulfide by single cation vacancies is insufficiently strong to explain the observed experimental regularities, in particular, the absence of conductivity sign inversion. The part of impurity ions becomes bind into the complexes with cation vacancies on bismuth concentration increase. The formation of complexes consisting of impurity atoms and vacancies along with the single vacancies can significantly reduce the energy of defects and thus considerably increase the self-compensation effect as well as change the character of dependence of the charge carrier concentration on the dopant impurity content. If consider that the bismuth impurity atoms are singly ionized Bi^- and the cation vacancies in GeS are doubly charged V_{Ge}^{++}, then the pairwise complexes $\{V_{Ge}$–Bi$\}$ are positively charged creating one charge carrier (hole) per one complex, wherewith the absence of conductivity type inversion is conditioned.

The introduction of Bi impurity atoms into germanium monosulfide leads to the appearance of high photosensitivity in the visible and near-infrared spectral ranges along with the increase of specific dark resistivity. The photosensitivity of bismuth-doped GeS crystals is by several orders of magnitude higher than the photosensitivity of intentionally undoped low-resistance crystals. So, the multiplicity of changes $\rho_{dark}/\rho_{light} = 10^3$ at 293 K and it reaches $\rho_{dark}/\rho_{light} = 10^4$–$10^5$ at low temperatures and illumination 10^4 lux.

The stationary photoconductivity spectra of high-resistance GeS crystals with different Bi impurity concentration are presented in Fig. 13 and 14. The PC spectra of slightly doped GeS crystals in addition to the intrinsic band-band maxima shows the impurity band with a maximum 1.34 eV and weak feature near intrinsic absorption edge with a maximum at 1.5 eV in $\boldsymbol{E} \parallel \boldsymbol{a}$ polarization (Fig. 13). There are observed the well-resolved maxima in the intrinsic absorption edge region of intentionally undoped GeS crystals while in this spectral region of heavily doped compensated GeS:Bi crystals (~1 at. % of impurity) it appears a wide continuum, the impurity band is broadened, its intensity increases and the energy position of its maximum is shifted to the lower energy region 1.3 eV.

The change of character of the spectral dependence of photosensitivity from the concentration of introduced Bi impurity into germanium monosulfide is naturally to associate with the change in the character of dissolution of impurity atoms in the matrix by increasing of their contents. As already noted above, the main mechanism of Bi impurity dissolution in GeS for the slightly doped crystals is filling the cation vacancies. At the filling of cation vacancies by impurity atoms in GeS crystal lattice in addition to vacancies the new type of defects appears – substitutional impurity defects which similar to vacancies lead to the formation of donor level in the bandgap (Fig. 7). The presence of impurity bands in PC spectrum with maxima at 1.34 and 1.5 eV is the confirmation of simultaneous presence in the bandgap of donor level created by bismuth impurity and acceptor level formed by the charged cation vacancies respectively (curve 2, Fig. 13). The estimation of donor level depth created by Bi impurity as the difference between the energies of intrinsic ($h\nu_{int}$ = 1.65 eV) and impurity ($h\nu_{imp}$ = 1.34 eV) maxima in the PC spectra give us the value 0.31 eV which is close to

the theoretically calculated 0.32 eV.

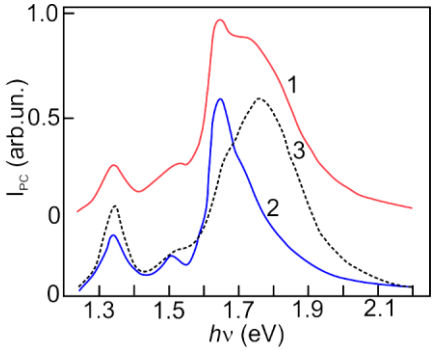

*Fig. 13. Unpolarized (1) and polarized (2, 3) photoconductivity spectra of GeS:Bi crystal (0.1 atomic % of Bi): 2 – **E** || **a**; 3 – **E** || **b**;. T = 293 K*

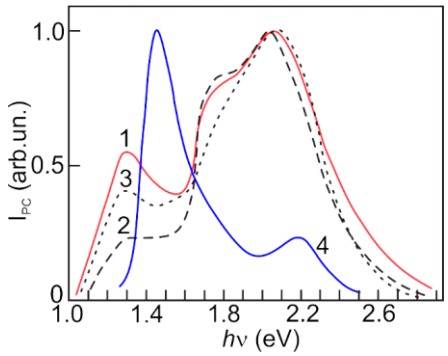

*Fig. 14. Unpolarized (1, 4) and polarized (2, 3) photoconductivity spectra of GeS:Bi crystal (1 atomic % of Bi): 2 – **E**||**a**; 3 – **E**||**b**; T: 1, 2, 3 – 293 K; 4 – 90 K*

The heavily doped compensated GeS:Bi semiconductor is an example of the disordered system because the chaotically located charged donors and acceptors create the large-scale fluctuations of electrostatic potential leading to the modulation of conduction band bottom and valence band top. Besides, the introduction of bismuth impurity atoms into GeS crystal lattice leads to the appearance of elastic stress fields caused by the difference of ionic atom radii of Ge^{2+} (0.73 Å) and Bi^{3+} (1.03 Å), and they can be easily amplified by inhomogeneous distribution of impurities. The presence of potential relief leads to the significant transformation of photoconductivity spectra both in the intrinsic and impurity regions (Fig. 14). The broadening and shift of intrinsic bands in the PC spectra to the lower energy region with the increasing of doping level of germanium monosulfide by bismuth can be qualitatively explained by a local decrease of band gap width due to "asymmetrical" curvature of conduction band and valence band at heavy doping.

Thus, the doping of germanium monosulfide by bismuth accompanied by the manifestation of a number of competing factors among which the next should be highlighted: the change in concentration of intrinsic cation vacancies (electroactive ones), the possibility of chemical interaction with the formation of complexes and the formation of fields of elastic distortions around the substitutional atoms.

The usage of the supercell approach allows calculating the electronic spectrum of germanium monosulfide both with a single impurity atom or with the high concentration of orderly located Bi impurity atoms. The calculation of electronic spectrum of Bi-doped GeS with arbitrary impurity concentration and arbitrary function of their spatial distribution in the lattice is currently complicated. Thus, as the possibilities to calculate of electronic spectra of heavily doped compounds currently are rather limited, then the experimental methods sensitive to the restructuring of electronic spectra of heavily doped semiconductors in comparison with the defect-free ones are stepped forward. As it follows from the presented results, the spectral distribution of photoconductivity rightfully belongs to the number of such experimental methods.

6. Conclusions

Performed in this paper study based on the density functional theory allowed to determine the character of change of GeS band structure at the presence of intrinsic point defects (vacancies in the cation and anion sublattices) as well as at the introduction of substitutional impurity (Bi→Ge) and at the formation of complexes $\{V_{Ge}+Bi_{Ge}\}$. It was established that the Coulomb interaction account (LDA+*U*-approximation) significantly affects the bandgap width and the depth of defect states in the comparison with the standard LDA-approximation.

It was performed the identification of observed features in the PC spectra of specially undoped and Bi-doped GeS crystals grown by the sublimation method based on the electronic structure calculation results of defect-free and defective germanium monosulfide. Substitutional Bi_{Ge} impurity with donor properties has the compensating effect on the intrinsic acceptor centers (V_{Ge}), causing the decreasing of concentration of free charge carriers (holes), and, as a result, it leads to the sharp increase of dark resistivity of GeS:Bi crystals without changing their conductivity type. Besides, Bi_{Ge} impurity substitutional atoms take the role of "sensitive" slow recombination centers responsible for the high integrated photosensitivity of doped crystals.

References

[1] D. I. Bletskan, V. I. Taran, M. Yu. Sichka, Ukrain. Phys. Journal **21**, 1436 (1976).
[2] P. P. Pogoretsky, E. N. Salkova, M. S. Soskin, D. I. Bletskan, I. F. Kopinets, USSR author's certificate, N 453976 (1974).
[3] D. I. Bletskan, I. F. Kopinets, P. P. Pohoretsky, E. N. Salkova, D. V. Chepur, Kristallograf. **20**, 1008 (1975).
[4] P. D. Antunez, J. J. Buckley, R. L. Brutchey, Nanoscale **3**, 2399 (2011).

[5] D. I. Bletskan, V. M. Kabatsii, Y. Y. Madyar, T. A. Sakal, Proceedings of IV International scientific-practical conference "Modern information and electronic technologies", Odessa, Ukraine, 276 (2003).
[6] C. Clemen, X. I. Saldaña, P. Munz, E. Bucher, Phys. Stat. Solidi (*a*), **49**, 437 (1978).
[7] D. I. Bletskan, N. V. Polazhinets, D. V. Chepur, Fiz. Tekhn. Poluprovodn. **17**, 1270 (1983).
[8] D. I. Bletskan, V. M. Kabatsii, Patent of Ukraine, Bul. **14**, N 106143 (2014).
[9] D. I. Bletskan, V. M. Kabatsii, M. M. Bletskan, Open Journal of Inorganic Non-Metallic Materials **6**, 7 (2016).
[10] D. I. Bletskan, V. M. Kabatsii, Patent of Ukraine, Bul. **12**, N 105856 (2014).
[11] D. I. Bletskan, Crystalline and glassy chalcogenides based on Si, Ge, and Sn, Part **1**. Binary and ternary systems, trad.: M. Popescu, Bucuresti, Editura INOE, Romania, 105, 2005.
[12] Th. Karakostas, J. Mater. Sci. **23**, 3099 (1988).
[13] D. I. Bletskan, Y. Y. Madyar, V. M. Kabatsii, Fiz. Tekhn. Poluprovodn. **40**, 142 (2006).
[14] T. Grandke, L. Ley, Phys. Rev. B. **16**, 832 (1977).
[15] F. M. Gashimzade, D. G. Guliev, D. A. Guseinova, V. Y. Shteinshrayber, J. Phys.: Condens. Matter **4,** 1081 (1992).
[16] L. Makinistian, E. A. Albanesi, Phys. Rev. B. **74**, 045206-1 (2006).
[17] Rathor, V. Sharma, N. L. Heda, Y. Sharma, B. L. Ahuja, Rad. Phys. Chem. **77**, 391 (2008).
[18] P. C. Kemeny, J. Azoulay, M. Cardona, L. Ley, Nuovo Cimento B. **39**, 709 (1977).
[19] Kosakov, H. Neumann, G. Leonhardt, J. Electr. Spectr. Relat. Phenom. **12**, 181 (1977).
[20] H. Neuman, A. Kosakov, Acta Phys. Polonica A. **55**, 779 (1979).
[21] R. B. Shalvoy, G. B. Fisher, P. J. Stiles, Phys. Rev. B **15**, 2021 (1977).
[22] R. B. Shalvoy, G. B. Fisher, P. J. Stiles, Phys. Rev. B **15**, 1680 (1977).
[23] G. D. Davis, P. E. Viljoen, M. G. Lagally, J. Electr. Spectr. Relat. Phenom. **21**, 135 (1980).
[24] T. Chassé, U. Berg, O. Brümmer, Phys. Stat. Sol. B **132**, 141 (1985).
[25] M. Taniguchi, R. L. Johnson, J. Ghijsen, M. Cardona, Phys. Rev. B. **42**, 3634 (1990).
[26] R. Eymard, A. Otto, Phys. Rev. B. **16**, 1616 (1977).
[27] Z. A. Jahangirli, Phys. Solid State **52**, 465 (2010).
[28] L. C. Gomes, A. Carvalho, A. H. Castro Neto, Phys. Rev. B **94**, 054103 (2016).
[29] H. Wiedemeier, H. G. Schnering, Z. Kristallogr. **148**, 295 (1978).
[30] R. A. Evarestov, Quantum chemistry of Solids, LCAO Treatment of Crystals and Nanostructures, 2nd Ed. Springer-Verlag Berlin Heidelberg, 2012.
[31] http://www.abinit.org/
[32] X. Gonze, J.-M. Beuken, R. Caracas, F. Detraux, M. Fuchs, G.-M. Rignanese, L. Sindic, G. Verstraete, G. Zerah, F. Jollet, M. Torrent, A. Roy, M. Mikami, Ph. Ghosez, J.-Y. Raty, D. C. Allan, Comp. Mat. Sci. B **25**, 478 (2002).
[33] http://departments.icmab.es/leem/siesta/
[34] J. M. Soler, E. Artacho, J. D. Gale, A. Garcia, J. Junquera, P. Ordejon, D. Sanchez-Portal, J. Phys.: Condens. Matter. **14**, 2745 (2002).
[35] C. Hartwigsen, S. Goedecker, J. Hutter, Phys. Rev. B **58**, 3641 (1998).
[36] N. Troullier, J. L. Martins, Phys. Rev. B **43**, 1993 (1991).
[37] J. Hubbard, Proc. R. Soc. London. Ser. A. **276**, 238 (1963).
[38] V. I. Anisimov, J. Zaanen, O. K. Andersen, Phys. Rev. B. **44**, 943 (1991).
[39] V. I. Anisimov, F. Aryasetiawan, A. I. Lichtenstein, J. Phys. **9**, 767 (1997).
[40] G. Valiukonis, G. Krivaite, D. I. Bletskan, A. Šileika, Phys. Stat. Sol. B **128**, K37 (1985).
[41] J. D. Wiley, D. Thomas, J. Phys. Chem. Solids. **41**, 801 (1980).

*Corresponding author: crystal_lab457@yahoo.com